A R C H I V E S O F M E T A L L U R G Y A N D M A T E R I A L S
Volume 60 2015 Issue 3
DOI: 10.1515/amm-2015-0397

J. FOURIE*,**#, J. LELITO*, P.L. ŻAK*, P.K. KRAJEWSKI*, W. WOŁCZYŃSKI***

NUMERICAL OPTIMIZATION OF THE GATING SYSTEM FOR AN INLET VALVE CASTING MADE OF TITANIUM ALLOY

NUMERYCZNA OPTYMALIZACJA UKŁADU WLEWOWEGO DLA ODLEWU ZAWORU DOLOTOWEGO ZE STOPU TYTANU

The main aim of this work was to numerically investigate and optimize feeding and geometrical parameters to produce inlet valves of Ti6Al4V alloy that are free from defects, especially porosity. It was found that the change of geometry orientation as well as inlet feeder diameter and angle showed distinct relationships between geometric alteration and occurrence of porosity. Alteration in the pouring parameters such as temperature and time had none or only slight effect on occurrence or position of porosity in the valve. It was also found that investigating individual parameters of simple geometry and then utilizing these best fit results in complex geometry yielded beneficial results that would otherwise not be attainable.

Keywords: numerical simulation; optimization; porosity, titanium alloys; investment casting; Ti6Al4V alloy; microstructure.

Głównym celem pracy były numeryczne badania i optymalizacja procesu zasilania oraz parametrów geometrycznych zaworów dolotowych ze stopu Ti6Al4V, zapewniających uzyskanie odlewów bez wad, w szczególności pozbawionych porowatości. Stwierdzono, iż zmiana położenia oraz średnicy i kąta pochylenia nadlewu pozostają w ścisłym związku z położeniem oraz kształtem pojawiającej się porowatości skurczowej. Zmiana parametrów zalewania form (temperatura, czas) nie ma, bądź ma niewielki wpływ na wystąpienie porowatości i jej lokalizację w odlewie zaworu. Stwierdzono, iż metoda badania wpływu poszczególnych parametrów procesu odlewania dla prostych kształtów, a następnie uogólnienie wyników najlepszych dopasowań na kształty złożone, daje korzystny wynik symulacji numerycznej, niemożliwy do uzyskania w inny sposób.

1. Introduction

In recent years the improvement of internal combustion engines through implementation of lighter and stronger materials has become a crucial factor in the development of motor vehicles. The combustion chamber of an internal combustion engine yields high temperatures in the range of up to 900°C [1-3]. The outlet valve is exposed to temperature in excess of 500°C and the inlet valve up to 350°C. Alternatively these components must withstand high pressure as well as aforementioned high working temperatures and Ti-6Al-4V alloy, an $\alpha - \beta$ alloy previously used for its high temperature properties and heat treatment possibilities fall into the category. Refer to Fig. 1 for a comparison of currently used materials for internal combustion engines and Ti6Al4V alloy. The Ti6Al4V alloy has significantly higher specific yield and ultimate tensile strength compared to other alloys, however, lower modulus of elasticity. The reduction in weight of these inlet valves has positive effects on the engine dynamics and overall fuel consumption. The lighter valves for example also has advantages down the line w.r.t. the requirement of lighter valves springs [4].

The Ti6Al4V alloy is also the most widely used titanium alloy at about 50% which makes well known to foundrymen and engineers [6]. A near-net-shape casting process must be investigated that would yield beneficial microstructural and mechanical results and yield completely sound components. The advantages of these near-net-shape components are reduced machining that reduces costs involved with lost material. Due to titanium's high cost near-net-shape casting offers the highest cost saving potential [5]. Due to the pouring conditions and titanium's affinity for oxygen and severe shrinkage during solidification of 3.5% [7], the most observed defect is porosity and for this reason porosity was exclusively investigated. Amendments to the geometry, initial – and boundary conditions were investigated to reduce

* AGH UNIVERSITY OF SCIENCE AND TECHNOLOGY, FACULTY OF FOUNDRY ENGINEERING, 23 REYMONTA STR., 30-059 KRAKOW, POLAND
** CAPE PENINSULA UNIVERSITY OF TECHNOLOGY, CAPE TOWN, SOUTH AFRICA
*** INSTITUTE OF METALLURGY AND MATERIALS, POLISH ACADEMY OF SCIENCES, 25 REYMONTA STR., 30-059 KRAKOW, POLAND
# Corresponding author: fourie@gmail.com

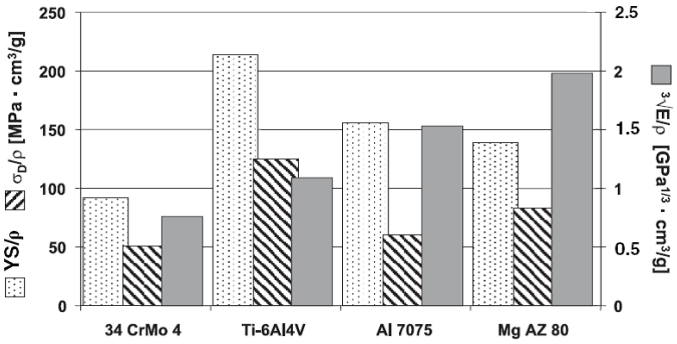

Fig. 1. Comparison of specific properties (Yield strength, Fatigue strength, Young's modulus) of a forged steel, Ti6Al4V alloy, a high strength aluminium alloy and high strength magnesium forged alloy [5]

the occurrence of porosity inside the component. The localised investigations were performed on a single feeder and component (Fig. 2). This process took into consideration the pouring and solidification process where factors such as shrinkage porosity and temperature gradients were analysed.

Fig. 2. Rendering of component with generic feeder

2. Experimental

The experimental material used for this investigation was Ti6Al4V due to its wide processing window and high temperature creep and corrosion resistant properties. The chemical composition of the alloy is 0.18% O_2, 0.015% N_2, 0.04% C, 0.006% H_2, 6% Al, 4% V and 0.13% Fe (by weight) [1]. The high aluminium and vanadium content also referred to as α-phase and β-phase stabilizers respectively provides a processing window that allows for a wide range of mechanical properties. Fig. 3 show a Scanning Electron Microscope image of 1000× magnification of a cast Ti6Al4V alloy. The grain size is on the order of 10 mm which represents the b-phase. The area plotted in the red square marked "1" in Fig. 3 is the b-phase and its composition is represented in Table 1. The a-phase is the small islands observed on the grain boundaries in Fig. 3 and Fig. 4. The area plotted in red square in Figure 4 represents the a-phase and this composition is represented in Table 2.

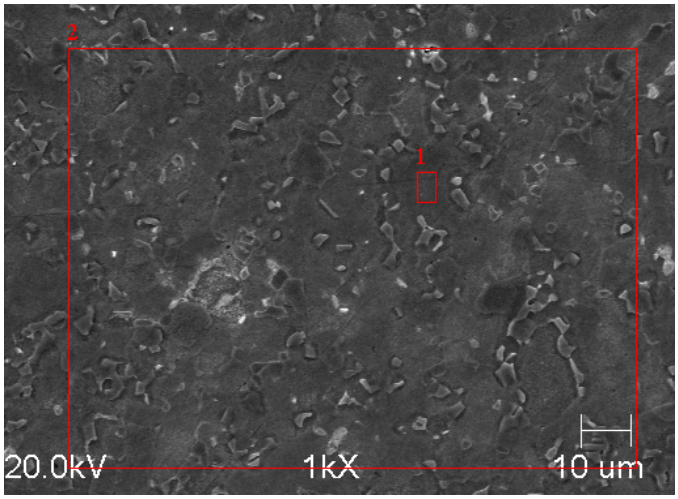

Fig. 3. SEM image representing the microstructure of a two phase titanium alloy, Ti6Al4V at 1000× magnification

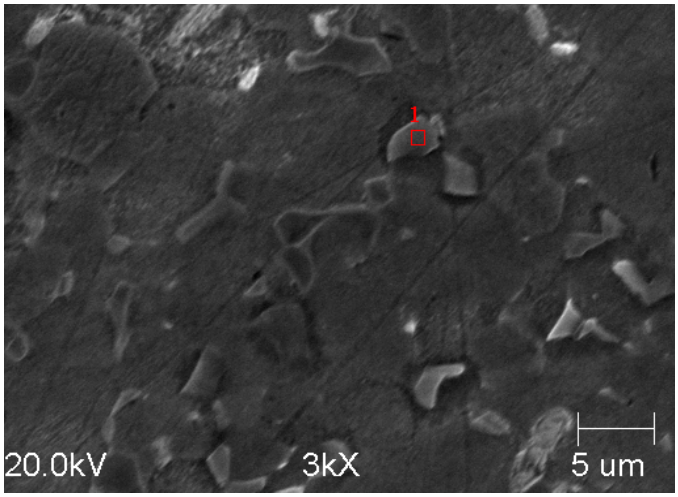

Fig. 4. SEM image representing the microstructure of a two phase titanium alloy, Ti6Al4V at 3000× magnification

TABLE 1

β-phase composition in Ti6Al4V alloy (as received)

Elt.	Line	Intensity (counts/s)	Error 2-sigma	Gauss Fit	at. %	wt. %	2-sigma	Error Int (counts/s)	Bkg Error 2-sigma	MDL 3-sigma
Al	Kα	62.69	3.21	2.57	11.013	6.513	0.334	7.3	0.986	0.222
Ti	Kα	743.72	10.091	5.26	87.519	91.827	1.246	10.03	1.157	0.309
V	Kα	10.16	1.827	3.37	1.276	1.425	0.256	7.43	0.995	0.302
Fe	Kα	0.99	1.002	0.2	0.192	0.235	0.237	3.27	0.66	0.339

TABLE 2

α-phase composition of Ti6Al4V alloy (as received)

Elt.	Line	Intensity (counts/s)	Error 2-sigma	Gauss Fit	at. %	wt. %	Error 2-sigma	Bkg Int (counts/s)	Bkg Error 2-sigma	MDL 3-sigma
Al	Kα	54.45	3.049	2.84	9.47	5.558	0.311	7.63	1.009	0.223
Ti	Kα	760.41	10.167	5.26	87.938	91.557	1.224	7.43	0.995	0.259
V	Kα	19.94	2.083	3.61	2.465	2.732	0.285	6.3	0.916	0.272
Fe	Kα	0.66	0.979	0.22	0.127	0.154	0.227	3.27	0.66	0.331

Figure 5 is an illustration of the final casting tree that should be successfully cast. The tree contains 48 components.

Fig. 5. Investment cast tree with 48 components

The investment casting tree illustrated in Fig. 5 was analysed by investigating only the individual component and its own inlet geometry, in this case inlet was a feeder. Fig. 2 shows the investigated valve with the cylindrical feeder connected to the head of the component. According to literature, porosity is the main defect observed in castings and for this reason it was decided to investigate amendments to the geometry, and initial and boundary conditions. Amendments made to these points previously mentioned and the effect to the properties of the component would be analysed. The localised investigations were performed on a single inlet feeder and component. This process took into consideration the pouring and solidification process where factors such as shrinkage porosity and cooling rate are analysed. This investigation was subdivided into nine distinct sub-categories as illustrated in Table 3.

It was determined that the most obvious area of interest was the head of the component (Fig. 6) due to the possibility of hot spots. These hot spots would create porosity if not fed adequately by metal during the solidification process [4,8]. Some factors that additionally contribute to the porosity in castings are shrinkage of the metal, gas removal, alloy composition, casting process, heating methods, temperature of mould, reactivity of mould with casting alloy and the pattern and gating system design [6,9]. Some of these factors are investigated in this study.

TABLE 3

Investigated cases and alterations performed

Case No.	Alterations performed to geometry and parameters
1	Component orientation from 0 to 90° in increments of 10°.
2	Length of inlet feeder from 5 to 23 mm in increments of 2 mm.
3	Change of diameter from 6 to 24 mm in increments of 2 mm.
4	Inlet feeder angle from 0 to 45° in increments of 5°.
5	Five shapes of inlet feeder.
6	Diameter of the insulation around the feeder from 24 to 36 mm in increments of 2 mm.
7	Initial inlet temperature from 1690 to 1740°C in increments of 5°C.
8	Feeding time from 1 to 4 s in increments of 0.25 s.
9	Mould temperature from 300 to 1000°C in increments of 50°C.

For each case and respective instance the measurements were taken and transferred to a spreadsheet and graph generator.

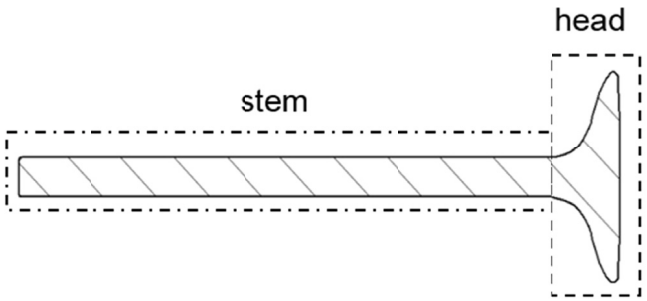

Fig. 6. Sections of component

For all cases, unless otherwise stated, the inlet temperature was 1740°C, initial mould temperature was 600°C, the component was orientated in a vertical position, the inlet diameter was 12 mm, the inlet length was 20 mm, inlet shape and angle was cylindrical and vertical respectively, feeding time was 2 seconds and no insulation was added to the inlet feeder or the component. Five thermocouples was placed along the centreline from the surface of the component head in 3 mm increments as shown in the Figure 7. The pouring procedure was performed under gravity and shielded from the atmosphere in a vacuum chamber.

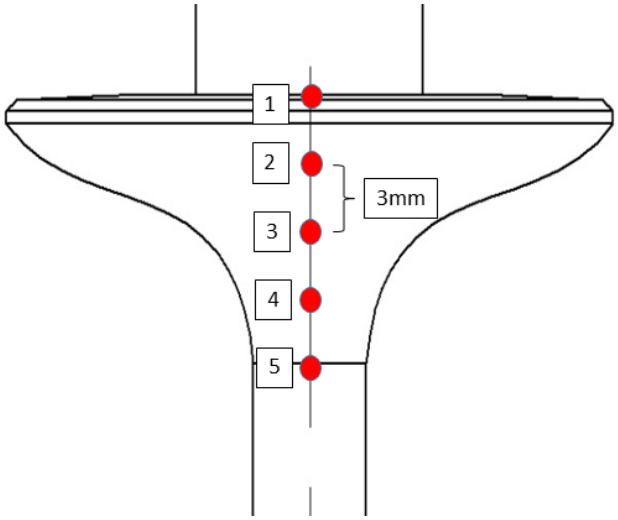

Fig. 7. Thermocouple locations inside the head of the component along the centreline

The porosity occurrence was interpreted making use of simple measuring devices such as a Vernier calliper and a ruler. The images obtained from MagmaSoft® were extracted and enlarged. A simple scaling algorithm was used to accurately measure occurrence and position of porosity up to 10^{-3} order of accuracy. For all subsequent graphs representing position of porosity vs. alteration the zero datum refers to the surface of the component head. Positive values refers to position of porosity inside feeder and negative values refers to position of porosity inside the component (refer to Fig. 8 for graphical representation).

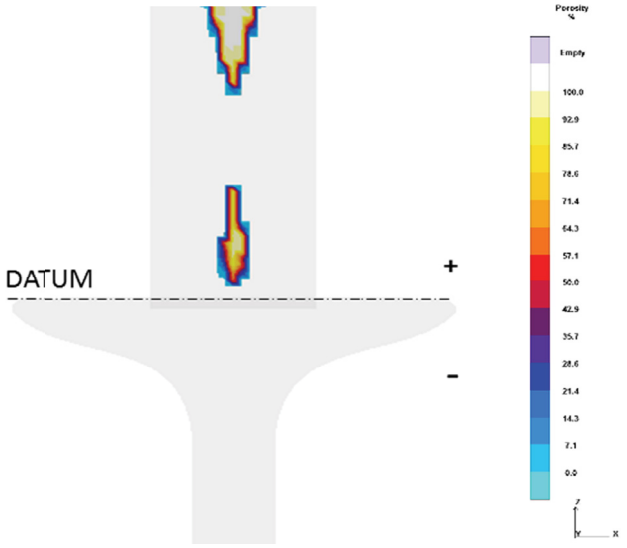

Fig. 8. Indication of datum line and positive and negative values in subsequent graphs

The results were then tabulated in a spreadsheet and relationships were investigated. The best fit results was then used in an optimized casting tree design to determine the validity of investigating individual parameters that influence casting and possibility of optimization of complex geometry.

3. Results and Discussion

3.1. Individual cases

Fig. 9 shows the relationship between the probability of porosity obtained from adjustment of the casting orientation w.r.t. the vertical one. It can be observed that the probability of porosity close to the surface of the head is dramatically reduced at utmost horizontal and vertical orientation. As the orientation is changed the relationship represents a parabolic function with the maximum value at 45° degrees. The same can be said for Fig. 10 that illustrates the position of porosity at the surface of the head. Here the vertical and horizontal positions again indicate the most favourable orientations with porosity at about 1 mm from the surface of the head located inside the feeder.

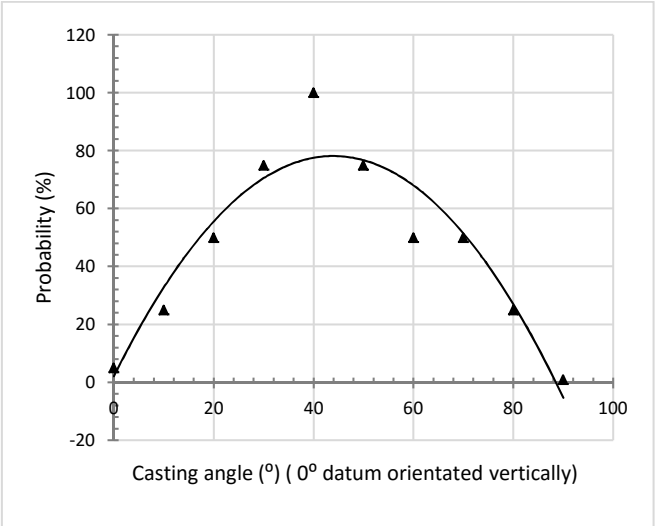

Fig. 9. Probability of porosity in component w.r.t. casting orientation

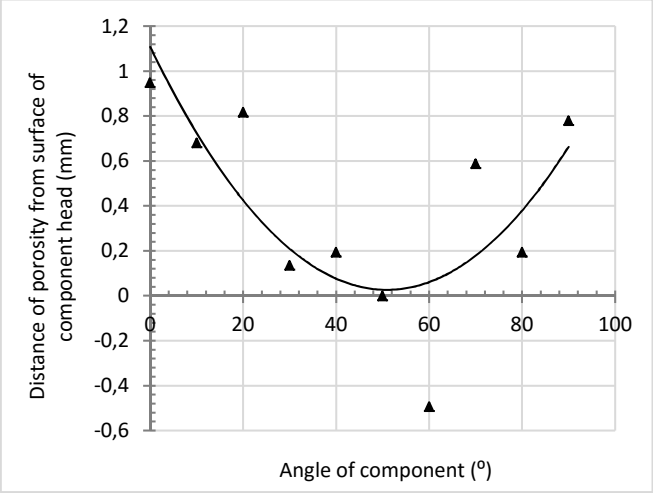

Fig. 10. Position of porosity w.r.t. the head of component vs. the orientation of component

Case number two investigated the feeder length and its relationship with position of porosity. The feeder length was

changed from 5 to 23 mm in 2 mm increments but no relationship was obtained, Fig. 11. However, according to [9] mould filling and mould filling time can be improved if the design of the gating system takes into consideration the shortest path in mind . It is therefore advantages to select the shortest length that would not produce porosity.

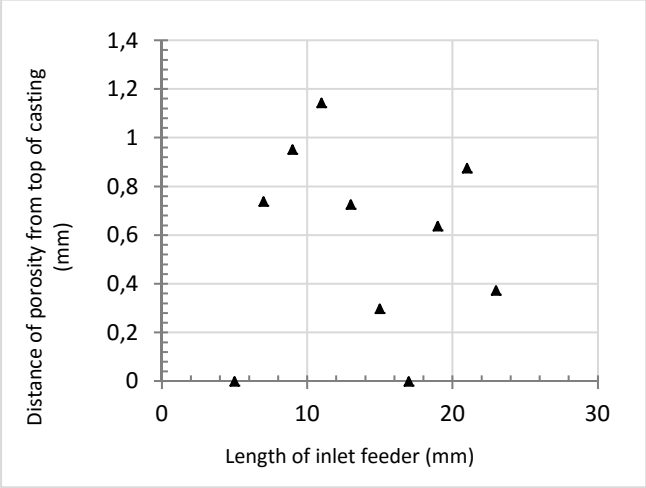

Fig. 11. Position of porosity w.r.t. the head of component vs. the length of the feeder

Fig. 12 illustrates the relationship obtained be changing the feeder diameter from 6 to 24 mm in 2 mm increments. A sigmoidal function can be observed and is illustrated in equation (1).

$$D = 11.5 + \frac{-15.5}{1+\left(\frac{d}{13.5}\right)^{10}} \quad (1)$$

where: D – distance from the surface of the head, mm; d – diameter of feeder, mm.

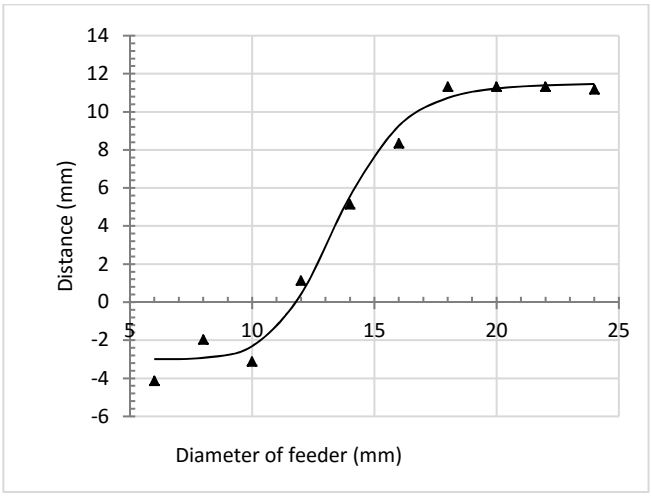

Fig. 12. Position of porosity w.r.t. the head of component vs. diameter of feeder

Porosity was observed in the feeder, on the surface and inside the head of the component for ϕ 6 mm feeder. As the diameter was increased the position of the porosity was altered and showed beneficial results. The relationship between the diameter and the position of porosity followed a generalised sigmoid function.

This slower cooling rate leads to longer cooling times at the surface of the component head. This effect could lead to microstructural changes that must be further investigated to determine the effect on mechanical properties (refer to Figs 13 and 14).

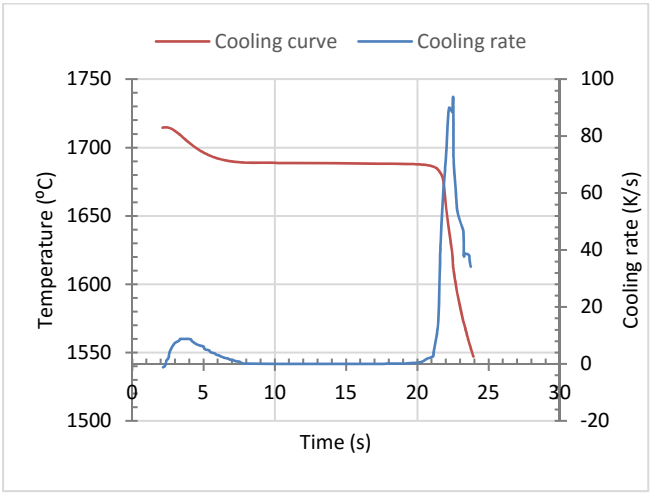

Fig. 13. Cooling curve and cooling rate for 14 mm diameter

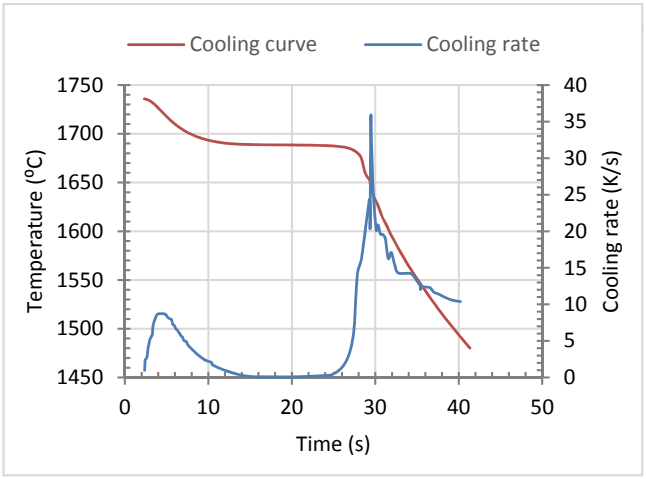

Fig. 14. Cooling curve and cooling rate for 22 mm diameter

In case five the inlet shapes was changed to consider the relationship between the shape and the occurrence and position of porosity. It was found that the spheroidal and pyramid shapes showed the best results as can be seen in Fig. 15. However, due to difficulty of manufacturing and assembly, these shapes were not used in the final design and the cylindrical shape was utilized.

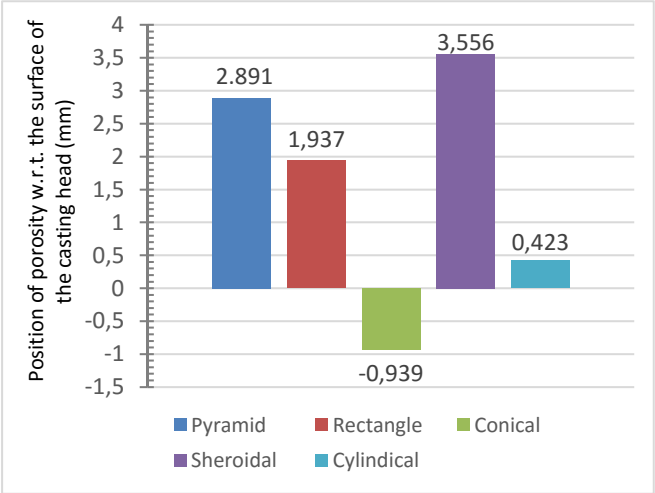

Fig. 15. Position of porosity vs. change of feeder shape

Fig. 16 shows the relationship between the changes of the feeder angle w.r.t. the casting orientation.

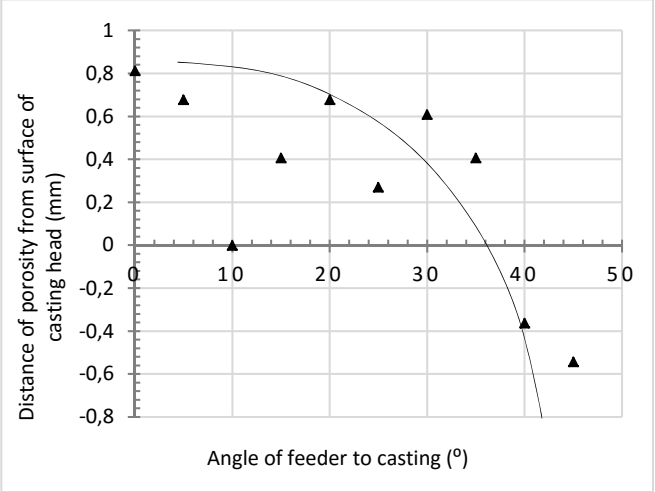

Fig. 16. Position of porosity w.r.t. the head of component vs. angle of the feeder to the casting head

As the angle is increased the tendency is for the porosity to 'move' towards the component surface head (negative gradient) as observed in proposed relationship in Fig. 16. The investigated range is less than 2 mm, and the results could therefore be a result of noise. The true relationship, if any, is not fully understood, but a tendency for porosity to move from the inlet feeder to the head of component is observed. Fig. 17 illustrates the linear relationship obtained when insulation was incorporated into the design of the casting. The outer diameter of the insulation was changed from 24 to 36 mm in 2 mm increments. No change to the position of the porosity was observed.

For case number seven the initial temperature to the inlet feeder was altered from 1690 to 1740°C in 5 degree increments to take into consideration the effect of temperature drop due to casting complexity and to probability of an altered temperature gradient. Fig. 18 illustrates that there is a positive tendency for the porosity to be removed from the surface of the component head. However, the change only occurred over an investigation area of 0.8 mm and results is therefore inconclusive.

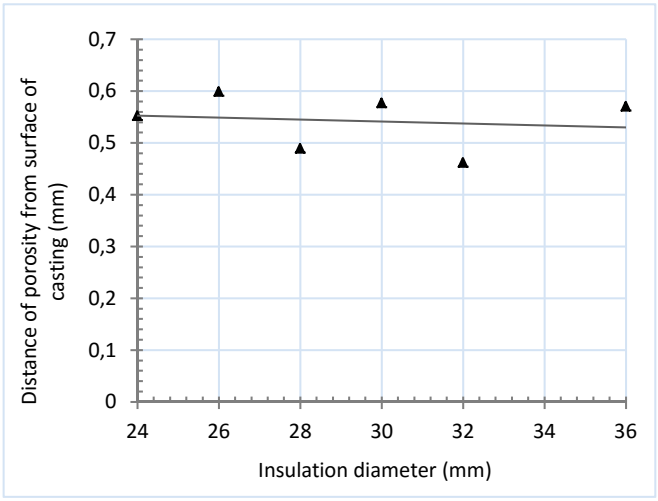

Fig. 17. Position of porosity w.r.t. the head of component vs. insulation diameter

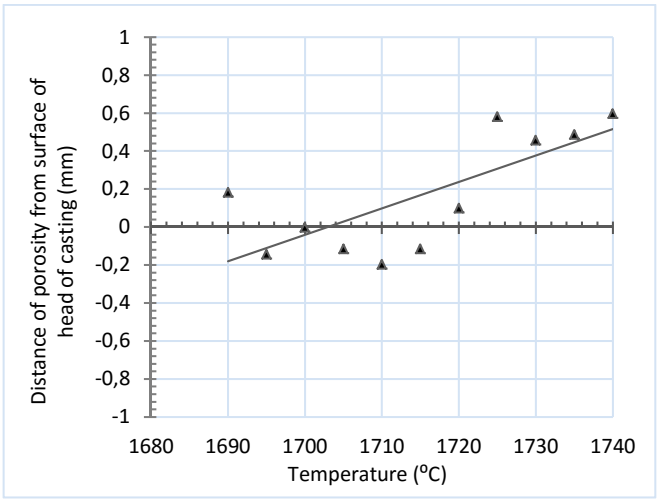

Fig. 18. Position of porosity w.r.t. the head of component vs. the inlet temperature

The temperature difference between molten metal and the mould material is too high costly miscasts can occur [5,8,10-11]. Some methods can also be employed to overcome these defects by superheating the alloy, but due to titanium's poor thermal conductivity it does not respond well to superheating processes [5]. It was concluded that a maximum pouring temperature of 1740°C was chosen as initial temperature as additional superheating would not yield beneficial results. The metal must also remain molten in areas that will solidify last to prevent hot spots and internal porosity [4,6].

For case number eight the feeding time was altered from 1s to 4s in 0.25 second increments, Fig. 19.

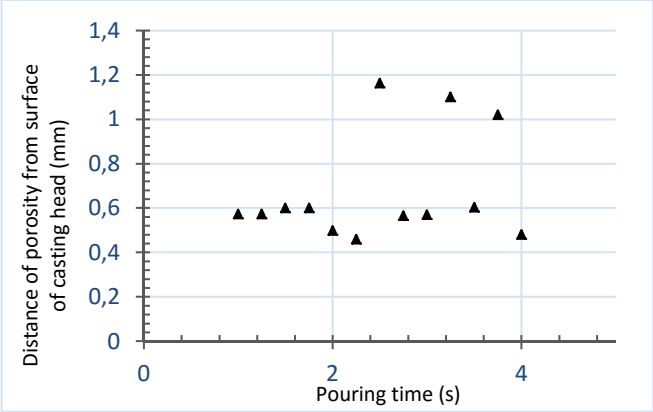

Fig. 19. Illustration indicating the effect of changing pouring time to the position of porosity w.r.t. the surface of the component head

No relationship was found for the range investigated between the change of inlet temperature and the position of porosity w.r.t. the surface of the component head. Titanium has unusual flow characteristics in molten state with poor thermal conductivity and rapid solidification [5,12-13]. It is suggested that the main reason for this is due to titanium's low density compare to other metals [13-15]. To overcome the rapid solidification of titanium the mould cavity must be filled rapidly [11]. Due to no effect to occurrence of porosity close to the head of the component the pouring time will be adjusted to be a rapid as possible.

For case nine data points was taken across the temperature range from 300 to 1000°C and the change of porosity was observed in Fig. 20.

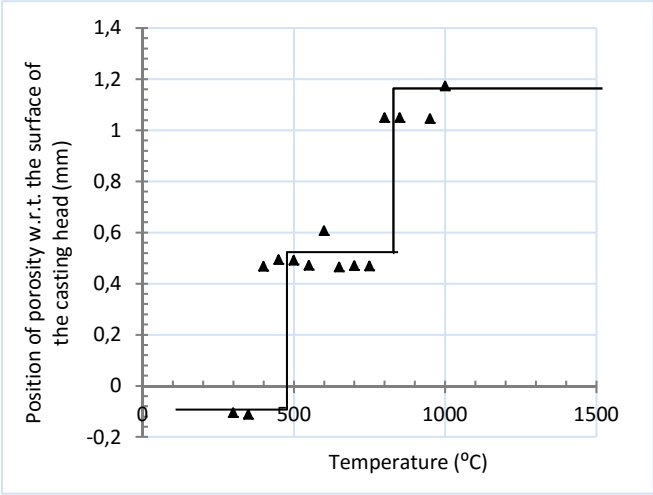

Fig. 20. Position of porosity w.r.t. the head of component vs. mould temperature

The recommended mould temperatures for casting titanium varies from room up to 600°C [10-11,14]. If the walls of the mould are too cold the walls will solidify first causing the walls to be impermeable and would stop the gasses from escaping. This would cause surface porosity resulting in poor surface quality. Alteration to the mould temperature shows a step function relationship across the range of 300 to 1000°C. The movement of porosity relative to the surface of the component head is rather insignificant with only a movement of 1.4 mm across a span of 700°C. Further increase of the mould temperature could yield further improvement, but according to literature and current study, a temperature of 600°C yields satisfactory results. Also the increase of mould temperature above an acceptable level becomes uneconomical. A 2-order polynomial relationship is observed in Fig. 21 for the solidification time of the component w.r.t. the change of mould temperature.

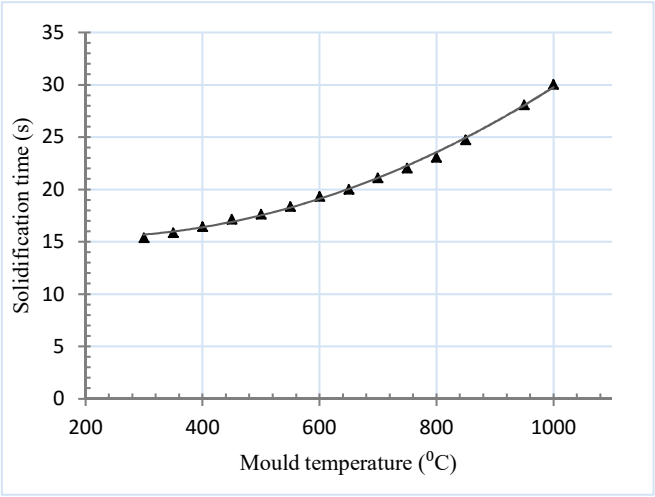

Fig. 21. Change of solidification time w.r.t. mould temperature

3.2. Final design

The final design was optimized using the best fit approach. The pouring temperature was 1740°C, the mould temperature was 600°C, the inlet orientation, length and diameter was vertical, 20 mm and 12 mm respectively, the inlet modulus was 3 mm, the pouring time was recalculated making use of turbulent flow calculations where maximum flow inside the mould should not exceed 1.5 m/s and was determined to be 12 seconds. The maximum yield obtainable from this casting tree is 30.8% and a total of 48 components was cast. After final casting tree was designed numerical simulations was performed. The option to investigate simulating the pouring and solidification process for the entire casting, as appose to making use of axis of symmetry, yielded pouring properties that would otherwise not have been observed. Overall soundness of the lower half of the casting tree (Fig. 22) can be observed in Fig. 23. No porosity or air inclusions are observed producing maximum yield, however, the upper half of the casting tree (refer to Fig. 24) showed signs of internal porosity in the stem that could be removed with HIP (High Isostatic Pressing) process if not severe. Signs of porosity at the surface and in the valve component head is not observed.

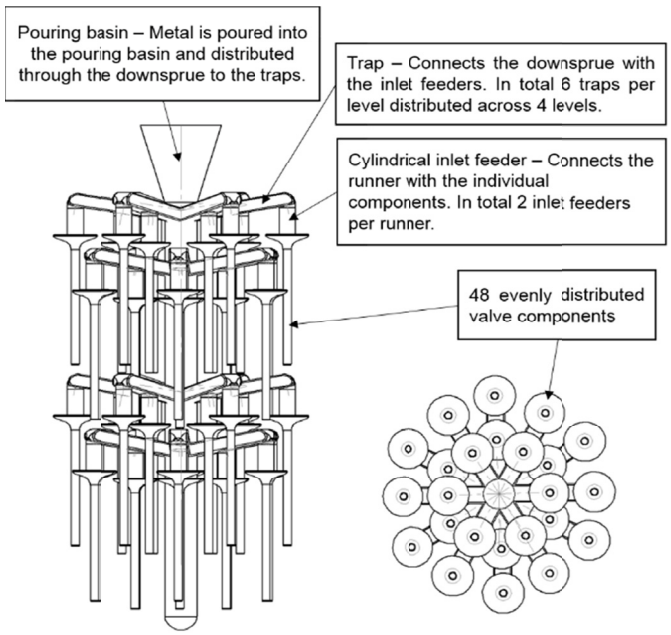

Fig. 22. Complete casting designed from individual investigates cases containing 48 components

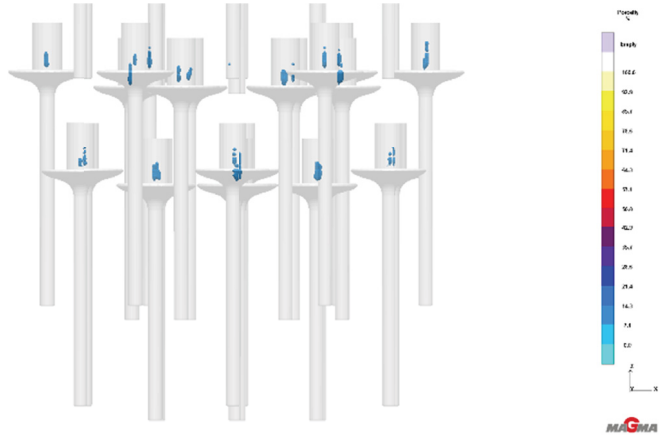

Fig. 23. Results obtained for the lower section of the complete casting tree indicating no porosity in component

Two distinct temperature groups are observed at the end of solidification (refer to Fig. 25). Casting numbers one, three, five and seven, orientated furthest away from the centreline and exposed to comparatively more ambient air, results in a final temperature of 160°C. Castings orientated closer to the centre-line and exposed to radiation from surrounding valves showed an average temperature increase of 40°C. This phenomenon is further described in Fig. 26 illustrating the cooling curves for each of these representative components of the casting tree.

The components located furthest away from the centreline yielded the highest cooling rates in the order of 100 K/s indicating the effect of ambient conditions on the surface. The components located on the closest to the centreline yield cooling rates in the order of 60 K/s.

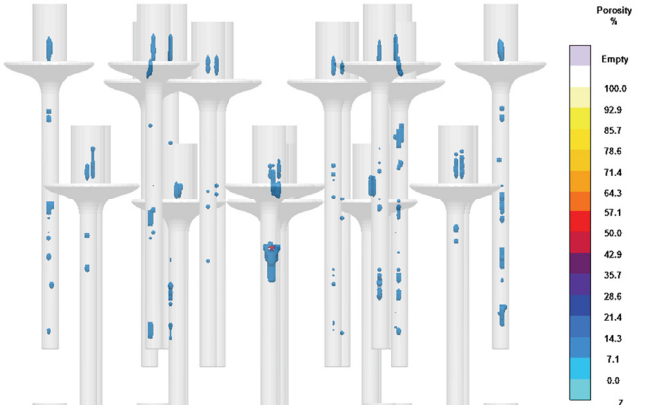

Fig. 24. Results obtained for the upper section of the complete casting tree indicating porosity distributed in the stem of the component

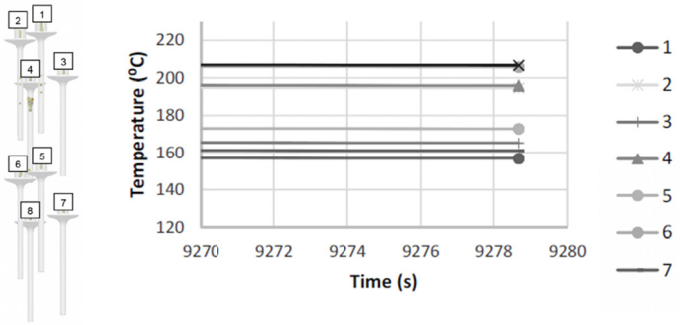

Fig. 25. Comparison of final temperature of each component as the final component solidified

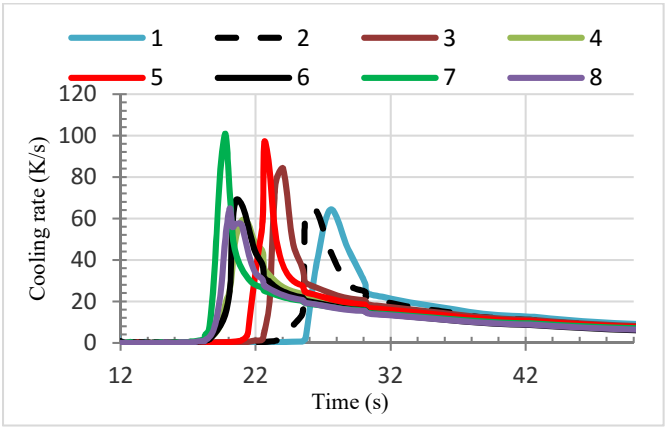

Fig. 26. Cooling rate for the reprehensive components for the casting tree

The complexity of the final casting tree yielded results not observed in the individually assessed components. The lack of metallostatic pressure in the upper half of the casting tree reduces pressure required to remove porosity and porosity is therefore observed in all the stems in the upper half. To improve the quality of the casting the casting must be performed under centrifugal force. The parameters in the individually investigated single casting set-up could successfully be employed in the

more complex design. Radiation plays a large role in the solidification of castings and must be investigated in future work to determine the extent of the effects. It should be also noted that such phenomena as grain refinement and back diffusion should be taken into consideration when casting structure, composition and technology are designing and/or numerically simulated [16-17]. For instance, the grain refinement through melt inoculation improves the feeding process of the solidifying castings and allows decreasing necessity of shrinkage porosity. The latter can be easily revealed in computer tomography examinations [18]. On the other hand, the back diffusion phenomenon strongly influences chemical composition of the structure arising during the cooling and solidification processes. Additionally using of insulating sleeves and, first of all, temperature dependencies of moulds thermophysical properties should be also taken into account [19-20].

4. Conclusion

From an experimental point of view this investigation showed that Ti6Al4V alloy can be successfully cast to an extent and optimized to produce a sound casting. It was observed that due to metallostatic pressure head of the casting orientated in the top half of the casting tree yielded unfavourable results. This shows that casting under gravity alone is not desired and the use of centrifugal casting for example would yield improved results. The individual parameters such as casting orientation, feeder diameter and angle, and mould temperature were altered and distinct relationships were observed. These relationships can be used for further optimization procedures and this numerical simulation should be experimentally reproduced. Final mechanical and microstructural properties must be found through mechanical tests and optical microscopy after which numerical optimization can be performed. The study showed that the individual parameters that influence the soundness of the casting can be investigated independently and then combined into a complex geometry that yields beneficial results. In 2000 Nissan Motor Company utilized valves made with Ti6Al4V alloy in one of their production vehicles with great success even though literature states that working temperatures inside the engine combustion chamber reaches temperatures exceeding safe working temperature of 350°C. The component is also not a complex shape, which is generally the governing reason for employing the investment casting process, although a sound casting was able to be produced. Investment casting is a process specifically for low volume high quality components that would be difficult or impossible to manufacture in any other way due to complexity, thin walls and type of material. Alterative manufacturing processes such as forging yields higher production numbers with consistent results. The rate at which these values can be produced using the investment casting process would not be sufficient for high production rates specifically in the automotive industry.

Acknowledgements

One of the authors (JF) would like to express sincere gratitude for financial support under RIFT scholarship from Cape Peninsula University of Technology, Cape Town, Republic of South Africa. The authors thank Faculty of Foundry Engineering – AGH UST for providing MagmaSoft software.

REFERENCES

[1] M.J. Donachie, Titanium. Materials Park, OH: ASM International (2000).

[2] V. Kazymyrovych, Very high cycle fatigue of engineering materials: A literature review, Karlstad University (2009).

[3] H. Voorwald, R. Coisse, M. Cioffi, Fatigue Strength of X45CrSi93 stainless steel applied as internal combustion engine valves. Procedia Engineering 10,1256-1261 (2011)

[4] L.G. Terkla, W.R. Laney, Partial Dentures. C.V. Mosby Co., Saint Louis, MO, 244-249(1963).

[5] H.G. Chung, M. Jean-Louis, T. Mori, Achieving high success rates in titanium casting using cold mold. Journal of Dental Research **73**, Abstract 2451, 408 (1994).

[6] C. Bessing, M. Bergman, The castability of unalloyed titanium in three different casting machines. Swedish Dentistry Journal 16, 109-113 (1992).

[7] O. Magnitskii, Casting properties of titanium alloys (1970.

[8] K.L. Stewart, K.D. Rudd, W.A. Kuebker, Clinical Removable Partial Prosthodontics. C.V. Mosby Co, St. Louis, MO, 357-358 (1983).

[9] K.F. Linefelder, C.W. Fairhurst, G. Ryge, Porosities in dental gold castings II. Effects of mold temperature, sprue size and dimension of wax pattern. Journal of American Dental Association **67**,816-821 (1963).

[10] H. Hero, M. Syverud, M. Waarli, Mold filling and porosity in castings of titanium. Journal of Dental Materials **9**, 15-18 (1993).

[11] K. Watanabe, S. Okawa, O. Miyakawa, S. Nakano, N. Shiokawa, M. Kobayashi, Molten titanium flow in a mesh cavity by the flow visualization technique. Journal of Dental Materials **10** (2), 128-137 (1991).

[12] R.I. Jaffee, M.E. Promisel, The Science, Technology and Application of titanium. Pergamon Press, New York, 5-17, 21-23, 79-84 (1970).

[13] J. Takahashi, J.Z. Zhang, M. Okazaki, Effect of casting method on castability of pure titanium. Journal of Dental Materials **12** (2), 245-252 (1993).

[14] M. Okazaki, H. Kimura, Reaction of titanium with trial phosphate-bonded investment molds. Journal of Dental Research **72**, Abstract 1426, 281 (1993).

[15] J.Z.Zhang, Effect of casting method on castability of pure titanium. Journal of Dental Materials **12**, (2), 245-252 (1993).

[16] J. Lelito, P.L. Żak, A.A. Shirzadi, A.L. Greer, W.K. Krajewski, J.S. Suchy, K. Haberl, P. Schumacher, Effect of SiC Reinforcment Particles on the Grain Density in a Magnesium Based Metal-

Matrix Composite: Modelling and Experiment, Acta Materialia **60**, 2950-2958 (April 2012).

[17] W. Wołczyński, W. Krajewski, R. Ebner, J. Kloch, The use of equilibrium phase diagram for the calculation of non-equilibrium precitipates in dendritic colidification theory, Calphad- Computer Coupling and Phase Diagrams and Thermochemistry **25**, 3, 401-408 (2001).

[18] W.K. Krajewski, J. Lelito, J.S. Suchy, P. Schumacher, Computed tomography – a new tool in structural examinations of castings, Archives of Metallurgy and Materials **54**, 335-338 (2009).

[19] W.K. Krajewski, J.S. Suchy, Determining Thermal Properties of Insulating Sleeves, Materials Science Forum **649**, 487-491 (2010).

[20] P.K. Krajewski, G. Piwowarski, P.L. Żak, W.K. Krajewski, Experiment and numerical modelling the time of a plate-shape casting solidification vs. thermal conductivity of mould material, Archives of Metallurgy and Materials **59**, 4, 1405-1408(2014).

[21] J. Lelito, P.L. Żak, A.L. Greer, J.S. Suchy, W.K. Krajewski, B. Gracz, M. Szucki, A.A. Shirzadi, Crystallization Model of Magnesium Primary Phase in the AZ91/SiC Composite, Composites: Part B **43**, 3306-3309 (2012).

Received: 20 April 2015.